



FLUCOME 2009

10th International Conference on Fluid Control, Measurements, and Visualization
August 17–21, 2009, Moscow, Russia

DIAGNOSTICS OF IMPULSE LINE BLOCKAGE WITH A MULTI-SENSING DIFFERENTIAL PRESSURE TRANSMITTER AT THE AIR LINE

Akira Uehara¹, Jun-ichi Eino², Takumi Hashizume³,
Tetsuya Wakui³, Nobuo Miyaji⁴, Yoshitaka Yuuki⁴

ABSTRACT

A differential pressure transmitter with an orifice is widely used as a flowmeter. A major drawback of this type of flowmeter is blockage of the impulse line, which connects the differential pressure transmitter to the orifice tap. A diagnostic method based on the amplitude of pressure fluctuations in the impulse line can be used to diagnose a blockage in the steady state; however, there is the possibility of an incorrect diagnosis in the transient state. This paper investigates the causes of this problem by comparing experimental results obtained at an air line with those obtained at a water line. In addition, the effectiveness of a diagnostic method that is based on the phase difference between the orifice high-side and low-side pressures is clarified in the transient state. It was observed that (1) long-term line pressure changes have harmful effects on the diagnosis of a blockage and (2) the diagnostic method can diagnose the blockage even in the transient state. However, this method cannot be used to diagnose severe blockage at an air line. Therefore, further improvement of the method is necessary.

Keywords: Diagnostic Technique, Fluctuating Pressure, Flowmeter, Compressible Flow, Differential pressure Transmitter, Impulse Line Blockage

INTRODUCTION

A differential pressure transmitter with an orifice, a so-called orifice flowmeter, is a common device that has been used for many years in process automation because it can be widely applied to various fluid lines. Orifice flowmeters are highly reliable, and only rarely experience problems. The most frequent problem is blockage of the impulse line, which connects the differential pressure transmitter to the orifice tap [1]. Ordinary periodic diagnostic tests and maintenance cannot usually detect impulse line blockage at the operation site. Therefore, an online diagnostic method to detect impulse line blockage is required.

In this study, we attempt to diagnose impulse line blockage by using a multi-sensing differential

¹ Corresponding Author: Research Institute for Science and Engineering, WASEDA University, email: uehara@power.mech.waseda.ac.jp, fax: +81-3-3203-3231

² Research Institute for Science and Engineering, WASEDA University

³ Department of Mechanical Engineering, OSAKA Prefecture University

⁴ YOKOGAWA Electric Corporation

pressure transmitter. In our previous studies, we suggested a diagnostic method that uses the high-frequency amplitudes of three pressure fluctuations—the orifice differential, as well as the high-side and low-side pressures [2][3]. This method is hereafter referred to as the diagnostic method based on the pressure fluctuations. We also suggest a diagnostic method that uses the delay of the phase difference between the high-side and the low-side pressures, hereafter referred to as the diagnostic method based on the phase difference[4]. We used both the diagnostic method based on the pressure fluctuations and the diagnostic method based on the phase difference to detect impulse line blockage at a water line and we observed that both the diagnostic methods were useful at any operating point (the line pressure and the flow rate) in the steady state. We also clarified the effectiveness of these two diagnostic methods in the transient state at the water line.

The purpose of this paper is to clarify the respective conditions in which our two proposed diagnostic methods are applicable to other fluid lines with different physical properties. Therefore, we applied the two diagnostic methods to an air line, which has small pressure fluctuations because of its compressibility. In addition, the effectiveness of these diagnostic methods in the transient state as well as in the static state is investigated by comparing the results obtained for an air line with those obtained for a water line.

EXPERIMENTAL INSTALLATIONS

A schematic diagram of our experimental installation at the air line is shown in Fig. 1. A compressor (0.69 MPa, 6.1 Nm³/min) supplies dry air to the test section through two tanks and a drier. The operating points are set by two valves—a ball valve set upstream of the orifice and a diaphragm control valve set downstream of the orifice. Furthermore, a schematic diagram of our experimental installation at the water line is shown in Fig. 2. A pump (1.2 m³/min, 100 m) supplies water to the test section through a pump outlet valve and a 100-mesh strainer. The operating point is controlled by a pump outlet valve and a diaphragm control valve set downstream of the orifice.

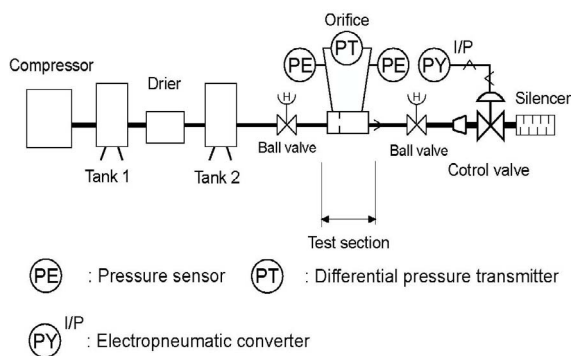


Fig. 1 Experimental installation (air line)

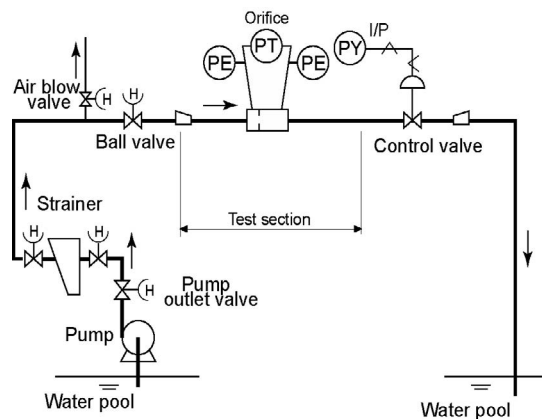


Fig. 2 Experimental installation (water line)

In each experimental installation, a function generator (Yokogawa Electric Corp.: FG120) is able to change the line pressure sinusoidally by generating sinusoidal voltage applied to an electro-pneumatic converter (Yokogawa Electric Corp.: PK200). Since the pressurized air supplied to the control valve is separated from the tested air line of Fig. 1, there are no harmful effects due to the control valve action on the flow of the tested air line.

Two schematic diagrams of the test sections—one at the water line and the other at the air line—are shown in Fig. 3. The orifice high-side and low-side pressures are separately transmitted to a differential

pressure transmitter through two stainless steel impulse lines (inner diameter: 6.0 mm, outer diameter: 8.0 mm, length: 1.8 m). In each impulse line, a needle valve (Fujikin Corp.: UN-14MB-S, rated Cv value: 0.015) is installed to simulate an impulse line blockage. Although there are various types of blockage conditions in an impulse line, this paper focuses exclusively on a local high-side blockage.

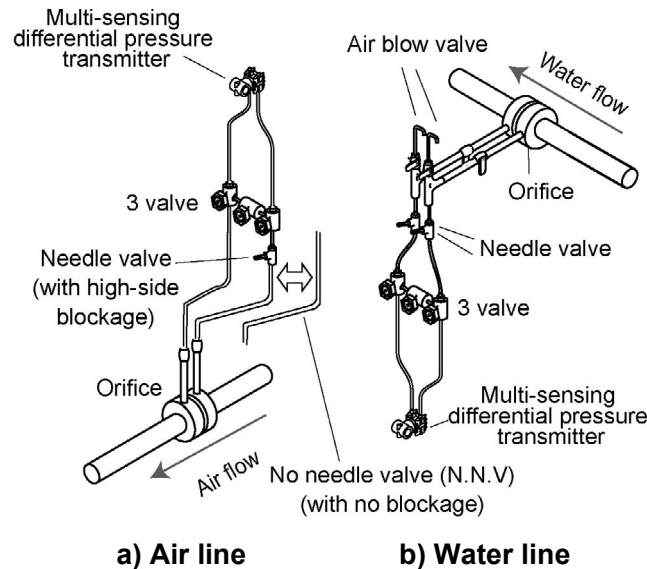


Fig. 3 Test section with high-side blockage

The needle valve opening is defined as the ratio of the current Cv value to the rated Cv value (0.015). In addition, the maximum valve opening (100%) is defined as a “no blockage” condition at the water line. However, the needle valve at the air line has a harmful effect on pressure transmission, even when the needle valve is set to the maximum valve opening (100%). Therefore, the impulse line without installing a needle valve is defined as a “no blockage” condition at the air line. Based on these no blockage conditions at the air line and at the water line, which are respectively defined above, the condition where the needle valve is set at the high-side impulse line is defined as a “high-side blockage” and the condition where the needle valve is set at the low-side impulse line is defined as a “low-side blockage”.

The tested differential pressure transmitter is of the multi-sensing type; it is able to measure three types of pressures—the differential pressure PD, the high-side pressure PH, and the low-side pressure PL—by using two resonant sensors on a silicon diaphragm[5]. The three pressures are calculated by using two measured oscillation frequencies of the resonant sensors, F_C and F_R . These frequencies, measured by using two frequency counters (Yokogawa Electric Corp.: TC110), are transmitted to a PC via GPIB (IEEE-488), as shown in Fig. 4. Although two oscillation frequencies are measured every 100 ms, additional 12 ms is required to transmit the signals to the PC. Thus, the sampling time of the frequency

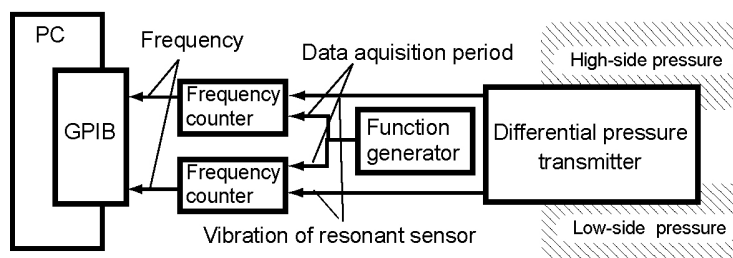


Fig. 4 Measurement system

counter is set to 112 ms by using a function generator (Yokogawa Electric Corp.: FG120). For the following experiments, the three pressures are measured for 5 min.

THE DIAGNOSTIC METHOD BASED ON THE PRESSURE FLUCTUATIONS

In our previous studies, we suggested a diagnostic method based on pressure fluctuations at the water line. The results revealed that this diagnostic method could be used to diagnose impulse line blockage before the blockage delayed pressure transmission. However, there is the possibility that not only the sensitivity of the diagnostic method but also the relationship between the pressure transmission delay and the valve opening at the water line are different from those observed in other fluid lines. Hence, in this study, we investigate the effectiveness of this diagnostic method at an air line by comparing the experimental results obtained at an air line with at a water line.

Determination of the Target Valve Opening for Diagnosing the Impulse Line Blockage

This subsection determines the target valve opening at the air line by clarifying the relationship between the pressure transmission delay and the valve opening. The pressure transmission delay is determined by the time constant when the air flow rate changes instantaneously. In this experiment, the line pressure is originally 220 kPa and the differential pressure is originally 25 kPa; this operating point is referred to as the original state. At the initial state, the operating points change from those mentioned above by closing the upstream ball valve so that the line pressure declines to 200 kPa and the differential pressure rises to 30 kPa. Then, the air flow rate is changed instantaneously from the initial state to the original state by opening the ball valve. The time constant in the response of the high-side and the low-side pressures to this change is defined as the time taken for the moving averages of the measured pressures, whose sampling number is 11, to reach 63.2% of its final value. Figure 5 shows the time constants at the air line and the time constant at the water line calculated in our previous study.

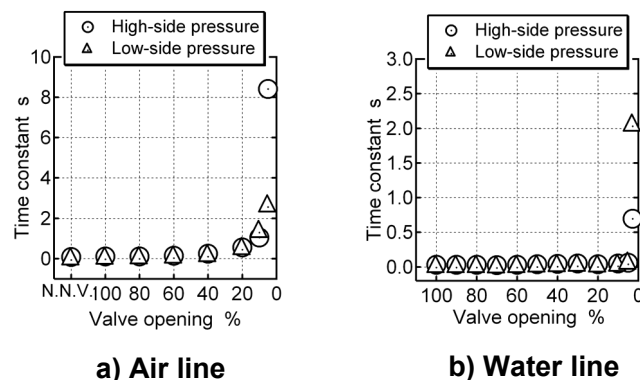


Fig. 5 Time constant

It is correct to say that the time constants of both the high-side and the low-side pressures at the water line increase in blockage when the valve is less than 40% open, as shown in Fig. 5-a). Our previous study determined that a time constant of more than 0.5 s is abnormal and we consider a valve opening of 5% as the target valve opening to diagnose impulse line blockage at the water line. Therefore, we consider a valve opening of 40%, which corresponds to a time constant of more than 0.5 s, as the target valve opening to diagnose impulse line blockage at the air line. Because each of these targeted valve openings is not a specific value that each fluid has, the targeted valve opening has to be investigated at each orifice flowmeter.

Effectiveness of the Diagnostic Method in the Steady State

For diagnosing the impulse line blockage before the targeted valve opening defined in the previous subsection, this subsection shows the effectiveness of the diagnostic method based on the pressure fluctuations in the steady state. In our previous studies, the amplitudes of the pressure fluctuations were quantitatively evaluated by using their root mean square (RMS) values. For example, Eq. (1) shows the RMS of the high-side pressure:

$$\text{RMS}_H = \sqrt{\frac{1}{N} \sum_{n=1}^N (P_{Hn} - P_{Hn+1})^2}, \quad (1)$$

where N is the total sampling number and P_{Hn} is the n_{th} measured high-side pressure. The total sampling number is about 2700 in this study.

This evaluation by using RMS is affected not only by impulse line blockage but also by a change in operating points. For this reason, we defined blockage indexes in order to diagnose the impulse line blockage without being affected by the change in operating points. The blockage index H is for a high-side blockage and L is for a low-side blockage, as shown in Eqs. (2) and (3):

$$H \equiv \frac{1}{N} \sum_{n=1}^N \frac{(P_{Hn} - P_{Hn+1})^2}{(P_{Ln} - P_{Ln+1})^2 + (P_{Dn} - P_{Dn+1})^2} \quad (2)$$

$$L \equiv \frac{1}{N} \sum_{n=1}^N \frac{(P_{Ln} - P_{Ln+1})^2}{(P_{Hn} - P_{Hn+1})^2 + (P_{Dn} - P_{Dn+1})^2}, \quad (3)$$

where P_{Hn} , P_{Ln} , and P_{Dn} are the n_{th} measured high-side, low-side, and differential pressures, respectively. Each blockage index was approximately 1 under the no blockage condition, and the index value of blocked-side impulse line decreased with an increase in the blockage. Therefore, these blockage indexes can be used not only to diagnose blockage but also to distinguish a high-side blockage from a low-side blockage.

Figure 6 shows the blockage indexes H and L under a high-side blockage condition at the air line and at the water line. The air line is in the steady state with a line pressure of 230 kPa and a differential

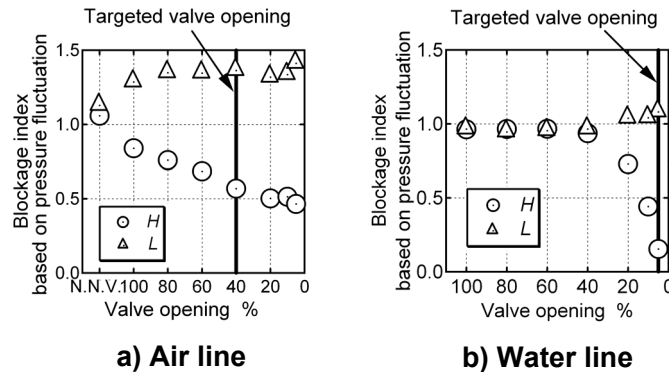


Fig. 6 Blockage index based on pressure fluctuations with high-side blockage in steady state

pressure of 10 kPa, while the water line is in the steady state with a line pressure of 550 kPa and a differential pressure of 50 kPa. The previous investigation at the water line set the sampling time of the differential pressure transmitter at 37 ms because of its high sensitivity. However, the pressure fluctuations at the air line, which are measured with a sampling time of 37 ms, are so small that the signal-to-noise ratio (S/N ratio) is very small. For this reason, the sampling times in this study are all 112 ms in order to compare the results of the air line with the results of the water line. Figure 6 shows that only the high-side blockage index decreases sufficiently with an increase in blockage that is less than the targeted valve opening shown by the solid line. These results show that the blockage indexes are able to diagnose blockage before the blockage delays pressure transmission in the steady state of each fluid line.

Effectiveness of the Diagnostic Method in the Transient State

The previous subsection investigated the effectiveness of the diagnostic method in the steady state. However, practical process lines are not always steady; some lines instantaneously change their operating points at start up, when changing the set points, and so on. Other lines continuously move their operating points to avoid valve sticking or to instantaneously feed water to a boiler. In addition, there is a possibility that an impulse line blockage changes the operating points continuously when the values measured by using the differential pressure transmitter are used as the controlled object. In our previous studies, we applied the diagnostic method based on the pressure fluctuations at a water line in which the line pressure changed continuously. The experimental results showed that this diagnostic method leads a incorrect diagnosis when the change in line pressure is large. To avoid an incorrect diagnosis, the degree of line pressure change was defined as an index of pressure variation (IPV), and the limit of this diagnostic method was quantitatively evaluated, as shown in Eqs. (4) and (5):

$$\text{IPV} \equiv \sqrt{\frac{\sum_{n=(M+1)/2+1}^{N-(M-1)/2} (\bar{P}_{Hn} - \bar{P}_{Hn})^2}{N - (M - 1)}} \quad (4)$$

$$\bar{P}_{Hn} = \frac{1}{M} \sum_{k=n-(M-1)/2}^{n+(M-1)/2} P_{Hk} , \quad (5)$$

where P_{Hk} is the k_{th} measured value of the high-side pressure and M is the number of sample for the moving average.

IPV shows the line pressure variation speed with regard to the sampling rate because IPV is the RMS of the moving averaged high-side pressure. In this paper, M is set to 41 on the basis of trial experiments. Therefore, IPV quantitatively evaluates the line pressure variation speed with a cycle length of over 5 s. Our previous studies involving the use of the diagnostic method based on the pressure fluctuations at a water line investigated the threshold IPV. At that time, we suggested that this diagnostic method should be suspended if the IPV was over the threshold value. However, the threshold IPV of another fluid line is still unclear. Therefore, this subsection investigates the threshold IPV where the diagnostic method based on the pressure fluctuations is available at the air line. By changing the control valve opening sinusoidally at the air line, we evaluate the decrease in the blockage index H with an increase in high-side blockage.

We investigate the relationship between the blockage index H and IPV at the air line and at the water line. Figure 7 shows the blockage index under two conditions, one in the no blockage condition and the other in the high-side blockage condition with targeted valve opening. The operating points of the air line

and the water line are respectively shown in Tables 1 and 2. Though the change in the line pressure is large, as shown in Tables 1 and 2, the flow rate is approximately constant.

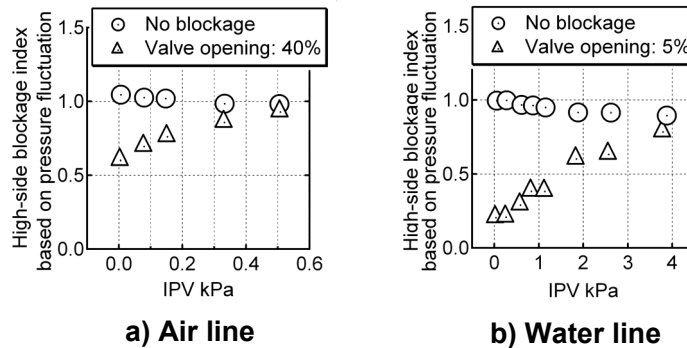


Fig. 7 High-side blockage index based on pressure fluctuation with high-side blockage in transient state

Table 1 Experimental condition of line pressure (air line)

IPV kPa	Offset kPa	Frequency Hz	Amplitude kPa
0	230	0	0
0.08	230	0.01	15
0.15	230	0.02	15
0.33	230	0.05	15
0.51	230	0.1	15

Table 2 Experimental condition of line pressure (water line)

IPV kPa	Offset kPa	Frequency Hz	Amplitude kPa
0	550	0	0
0.3	550	0.02	50
0.6	550	0.05	50
0.9	550	0.1	50
1.2	550	0.02	100
1.8	550	0.1	60
2.6	550	0.05	100
3.9	550	0.1	100

When the IPV is 0 kPa, that is, when it is in the steady state, the difference between the values of H under the no blockage condition and under the high-side blockage condition is large at the air line as well as at the water line. However, the more IPV increases, the smaller is the difference between the values of H under the no blockage condition and under the high-side blockage condition. Particularly, when the IPV at the air line is over 0.1 kPa and when the IPV at the water line is over 3 kPa, the difference between the values of H under the no blockage condition and under the high-side blockage condition is smaller than 0.2, so that it is difficult to diagnose the impulse line blockage.

In order to investigate the cause of these problems, the relationship between the RMSs under the no blockage and the high-side blockage conditions with targeted valve openings are shown in Figures 8 and 9. These results show that the RMSs of the high-side and the low-side pressure increase with an increase in the IPV, regardless of the fluid line. This is because long-term line pressure change is quantitatively evaluated as the RMS when the IPV is much larger than the amplitude of the pressure fluctuations. On the other hand, the IPV does not have a large effect on the RMS of the differential pressure because the differential pressure changes with an increase in the IPV. In addition, when the IPV increases, the RMS of the high-side pressure is larger than the RMS of the differential pressure under the high-side blockage, even though the RMS of the high-side pressure in the steady state is smaller than the RMS of the differential pressure under a high-side blockage.

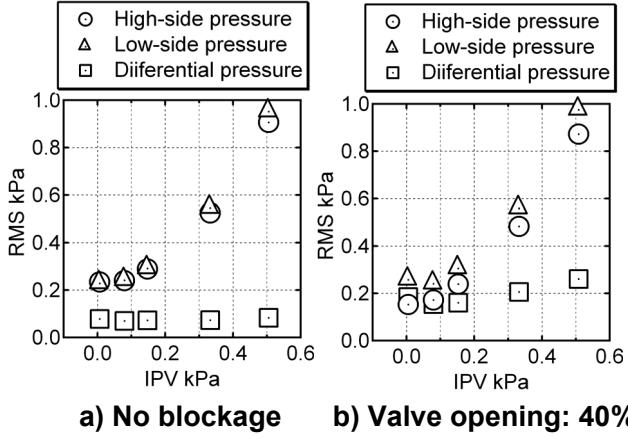


Fig. 8 Relation between RMS and IPV (air line)

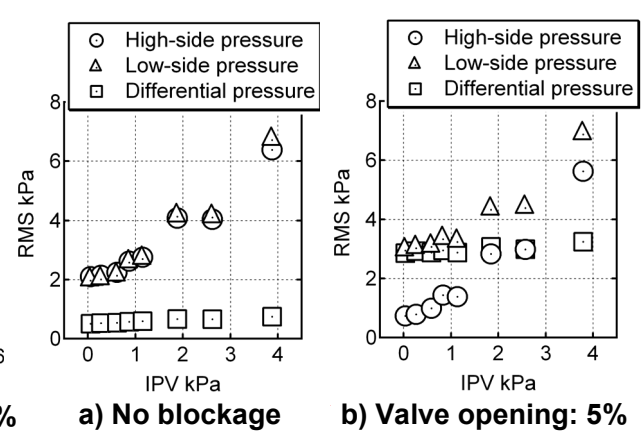


Fig. 9 Relation between RMS and IPV (water line)

These experimental results in the transient state show that the diagnostic method based on the pressure fluctuations is useful only when the amplitudes of the high-side and the low-side pressure fluctuations are much larger than the IPV. In addition, each fluid line has a different threshold IPV where the blockage indexes are available because the threshold IPV depends on the amplitude of the high-side and the low-side pressure fluctuations in each line.

THE DIAGNOSTIC METHOD BASED ON THE PHASE DIFFERENCE

This section applies another diagnostic method to the air line that is useful regardless of the amplitude of pressure fluctuations and the IPV—the diagnostic method based on the phase difference. In addition, the effectiveness of this diagnostic method in the transient state is investigated by comparing the experimental results at the air line with those obtained at the water line.

Blockage Index Based on Phase Difference

The diagnostic method based on the phase difference diagnoses an impulse line blockage by quantitatively evaluating the delay of the transmission of pressure fluctuations through two impulse lines. This subsection reports a new blockage index that employs the phase difference. Figure 10 shows the calculation flow of this diagnostic method. First, the power spectral densities and the phase differences between the high-side and the low-side pressures are calculated by using FFT. The phase difference is defined as in Eq. (6) at all frequencies:

$$\Delta\phi(f) \equiv \phi_H(f) - \phi_L(f), \quad (6)$$

where $\Delta\phi(f)$ in degrees is the phase difference of the pressure transmission at f Hz, $\phi_H(f)$ in degrees is the phase of the high-side pressure at f Hz, and $\phi_L(f)$ in degrees is the phase of the low-side pressure at f Hz. Since the measurement continues for 5 min, the base frequency f_0 is 3.3×10^{-3} Hz. The maximum frequency f_s is 4.5 Hz because the sampling rate is 112 ms. Second, in order to detect the blockage accurately, the frequencies, at which the phase differences are scattered, are eliminated as described below.

The averaged power spectral density of the high-side pressure and the low-side pressure is calculated from Eq. (7):

$$\overline{\text{PSD}} = \exp\left(\frac{1}{f_s/f_0} \sum_{i=1}^{f_s/f_0} \ln(\text{PSD}(if_0))\right), \quad (7)$$

where $\text{PSD}(if_0)$ is the power spectral density at $i \times f_0$ Hz.

Those frequencies, at which the power spectral densities of the high-side pressure or the low-side pressure are less than the averaged power spectral densities of each, are eliminated, and the phase difference corresponding to the frequencies, at which the power spectral density is not eliminated, is then evaluated.

The remaining phase difference is classified to either the positive side (0 to 180 deg) or to the negative side (0 to -180 deg).

Finally, the blockage index based on the phase difference (BIP) is calculated as shown in Eq. (8):

$$\text{BIP} = S_{\phi_-} / S_{\phi_+}, \quad (8)$$

where S_{ϕ_-} is the number of the negative phase difference and S_{ϕ_+} is the number of the positive phase difference. Under the no blockage, high-side blockage, and low-side blockage conditions, the BIP is approximately 1, more than 1, and less than 1, respectively.

Blockage Detection in the Transient State

This subsection applies BIP to the air line and to the water line, the operating points of which are shown in Tables 1 and 2. Figure 11 shows the BIPs under the no blockage condition and a high-side blockage in the transient state. The BIP of each fluid line increases from 1 to more than 4 with an increase

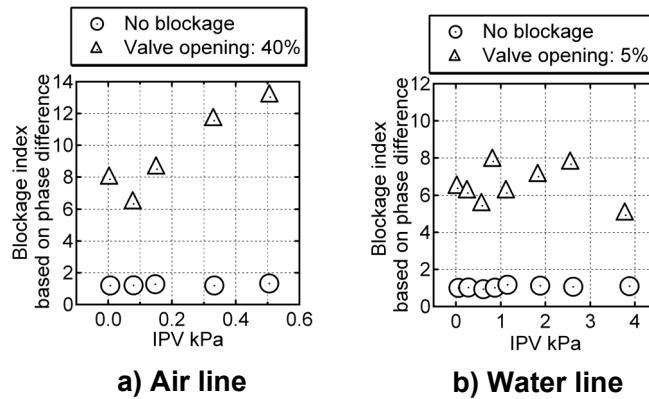


Fig. 11 Blockage index based on phase difference with high-side blockage in transient state

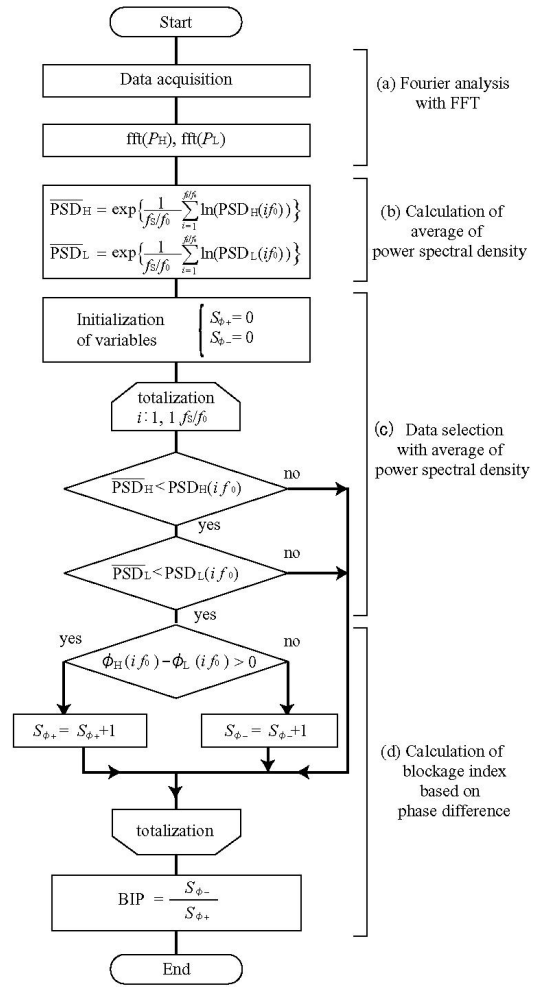


Fig.10 Calculation flow of blockage index based on phase difference.

in the high-side blockage. Particularly, Fig. 11-a) shows that the BIP under a high-side blockage at the air line increases with an increase in the IPV. This is because the average of the power spectral densities is used for elimination. Figures 12 and 13 show the phase difference and the power spectral density of the high-side pressure at the air line in the static state. In addition, Figs. 14 and 15 show the phase difference and the power spectral density of the high-side pressure at the air line in the transient state (IPV: 0.51). Figures 12 and 14 shows that the phase differences under the no blockage condition are concentrated around 0 deg, and the phase difference under the high-side blockage (targeted valve opening) is distributed to the negative side regardless of the IPV. On the other hand, Figs. 13 and 15 show that the high-side power spectral density at a low frequency increases with an increase in the IPV. This increase in the high-side power spectral density at low frequency affects the elimination of the phase difference. Particularly, the S/N ratio at the air line is so small that the average of the power spectral density eliminates more phase differences than at the water line. Therefore, the BIP at the transient state distinguishes the no blockage condition from the high-side blockage more accurately than at the steady state.

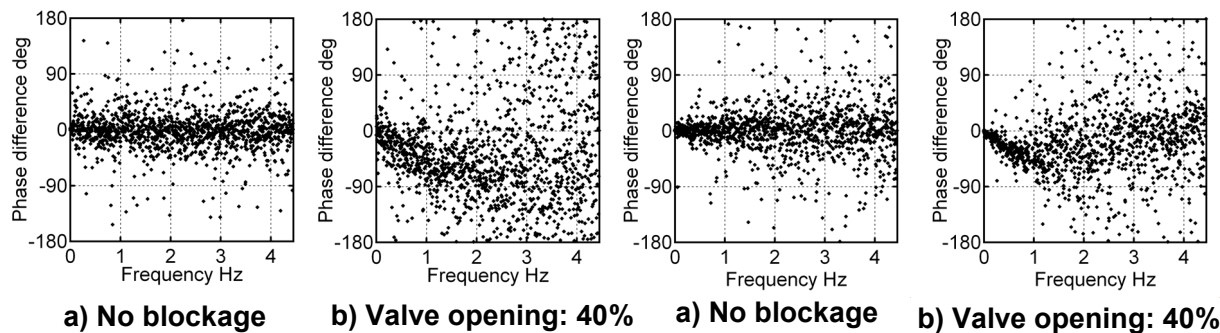


Fig.12 Phase difference distribution with high-side blockage in steady state (air line)

Fig.14 Phase difference distribution with high-side blockage in transient state (IPV: 0.51, air line)

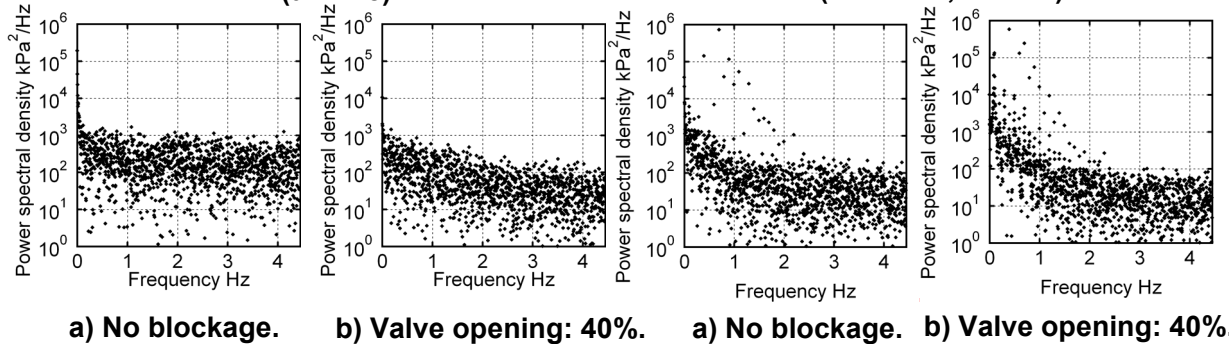


Fig.13 Power spectral density of high-side pressure with high-side blockage in steady state (air line)

Fig.15 Power spectral density of high-side pressure with high-side blockage in transient state (IPV: 0.51, air line)

The Effectiveness of the Diagnostic Method Based on the Phase Difference

This subsection investigates the effectiveness of the diagnostic method based on the phase difference under blockage conditions. Figure 16 shows the BIP under the same condition as Fig. 6. The BIP at the water line increases with an increase in the blockage. However, the BIP at the air line decreases below a valve opening of 40%, though the BIP above 60% increases with an increase in blockage. This is because a severe blockage weakens the correlation between the high-side and the low-side pressure fluctuations.

Figure 17 shows the power spectral density and the phase difference under a high-side blockage, where the valve opening is 0% at the air line. This result shows that pressure is not very well transmitted through the severe blockage. Therefore the common mode noises of the measurement system of both sides of the differential pressure transmitter have concentrated the phase difference at 0°.

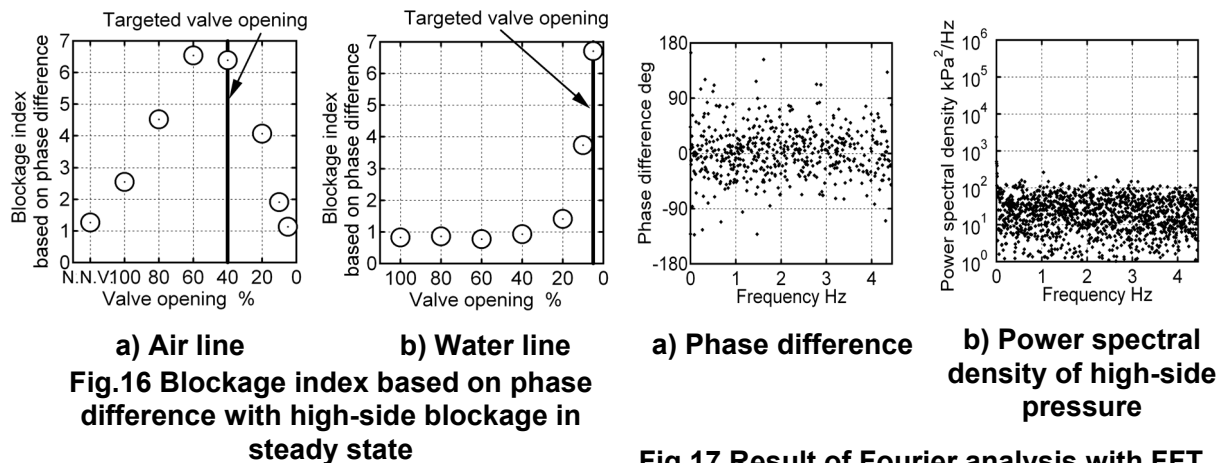


Fig.16 Blockage index based on phase difference with high-side blockage in steady state

Fig.17 Result of Fourier analysis with FFT with high-side blockage in steady state (valve opening: 0%)

In order to distinguish the no blockage condition from the severe blockage condition, the phase-difference method was used to evaluate the correlation between the high-side and the low-side pressures. For example, this correlation is evaluated by the following equation by using the coherence function of MATLAB:

$$C_{HL}(f) = \frac{|\text{PSD}_{HL}(f)|^2}{\text{PSD}_H(f)\text{PSD}_L(f)}, \quad (9)$$

where $C_{HL}(f)$ is the coherence function at frequency f Hz, $\text{PSD}_{HL}(f)$ is the cross-spectral density of the high-side and the low-side pressure, $\text{PSD}_H(f)$ is the power spectral density of the high-side pressure, and $\text{PSD}_L(f)$ is the power spectral density of the low-side pressure.

Figure 18 shows the coherence between the orifice high-side and low-side pressure under the no blockage condition and the severe high-side blockage (valve opening: 5%) in the steady state at the air

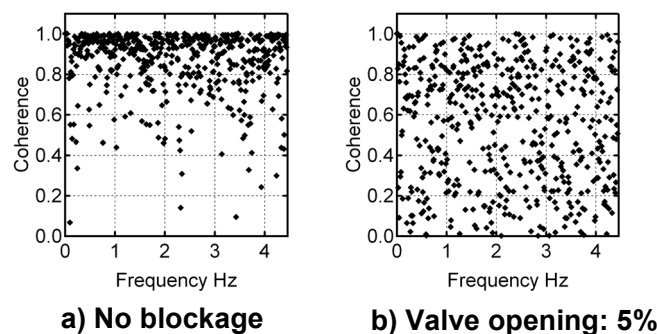


Fig. 18 Coherence between orifice high-side and low-side pressure with high-side blockage in steady state

line. Figure 18-a) shows that the coherence under the no blockage condition is concentrated at 1. On the other hand, Fig. 18-b) shows that the coherence under the severe blockage condition is scattered from 0 to 1. In the next study, we will add an evaluation of the correlation between the high-side and the low-side pressure to the diagnostic method based on the phase difference in order to diagnose severe blockage.

CONCLUSION

This study investigates the effectiveness of two diagnostic methods, the diagnostic method based on the pressure fluctuations and the diagnostic method based on the phase difference. This paper aims to clarify the effectiveness of the diagnostic methods in both the steady state and in the transient state by applying these methods to a water line and to an air line.

The experimental results show that the diagnostic method based on the pressure fluctuations is useful in the steady state. However, it is necessary to suspend the diagnostic method when long-term line pressure changes are larger than the amplitude of the pressure fluctuations. Therefore, when the line has small pressure fluctuations, like the air line, even the small line pressure change causes a loss of diagnostic ability of the pressure-fluctuation method.

The phase-difference method, however, is able to diagnose an impulse line blockage regardless of long-term line pressure changes. However, this diagnostic method relies on a correlation between the high-side and the low-side pressures, so this method can not distinguish a severe blockage from a no blockage condition. In the next study, we will develop the diagnostic method further, including the evaluation of the coherence between the high-side and the low-side pressure.

REFERENCES

- [1]Sento, T. (1999), “Impulse Line less Measurement Using Remote Seal Type Differential Pressure Transmitter vs. Impulse Line less Measurement with Direct-mount (in Japanese)”, KEISO, 42 (2), 32–36.
- [2]Eino, J., Wakui, T., Hashizume, T., Miyaji, N., Saito, Y., Nishijima, T. and Kuwayama, H. (2006), “Detection of impulse line blockage using a digital differential pressure transmitter,” Proceedings of the 19th International Congress COMADEM '06, 425–434.
- [3]Eino, J., Wakui, T., Hashizume, T., Miyaji, N., Kuromori, K., Yuuki, Y. (2007), “Diagnostics of Impulse Line Blockage in Water Line with Transient State,” Proceedings of the FLUCOME 2007, CD-ROM, No.53.
- [4] Eino, J., Uehara, A., Wakui, T., Hashizume, T., Miyaji, N., Yuuki, Y. (2008), “Monitoring of Impulse Line Blockage using Phase Difference between Upstream and Downstream Pressures of Orifice,” Proceedings of the ASME Power 2008, CD-ROM.
- [5]Ishikawa, T., Otohira, T., Nikkuni, M., Koyama, E., Tumagari, T., Asada, R. (2004), “New DPharp EJX Series Differential Pressure and Pressure Transmitters (in Japanese)”, Yokogawa Technical Report, Japanese Edition, Vol.48, No.1, 13-18.